Journal of Computer-Aided Molecular Design, **13:** 409–418, 1999.
KLUWER/ESCOM

Analysis of Fas–ligand interactions using a molecular model of the receptor–ligand interface

Jürgen Bajorath[a,b,*]
[a]*MDS Panlabs, Computational Chemistry & Informatics, 11804 North Creek Pkwy. S., Bothell, WA 98011-8805, U.S.A.*
[b]*Department of Biological Structure, University of Washington, Seattle, WA 98195, U.S.A.*

Received 28 August 1998; Accepted 11 November 1998

Key words: comparative modeling, contact residues, Fas (CD95)-ligand interactions, structural conservation, TNFR/TNF-β complex

Summary

A molecular model of the complex between Fas and its ligand was generated to better understand the location and putative effects of site-specific mutations, analyze interactions at the Fas–FasL interface, and identify contact residues. The modeling study was conservative in the sense that regions in Fas and its ligand which could not be predicted with confidence were omitted from the model to ensure accuracy of the analysis. Using the model, it was possible to map four of five N-linked glycosylation sites in Fas and FasL and to study 10 of 11 residues previously identified by mutagenesis as important for binding. Interactions involving six of these residues could be analyzed in detail and their importance for binding was rationalized based on the model. The predicted structure of the Fas–FasL interface was consistent with the experimentally established importance of these residues for binding. In addition, five previously not targeted residues were identified and predicted to contribute to binding via electrostatic interactions. Despite its limitations, the study provided a much improved basis to understand the role of Fas and FasL residues for binding compared to previous residue mapping studies using only a molecular model of Fas.

Introduction

Fas (CD95) [1] and its ligand (FasL) [2] are members of the tumor necrosis factor (TNF) receptor (TNFR) superfamily (TNFRSF) [3] and the TNF superfamily (TNFSF) [4], respectively. These protein families consist of transmembrane proteins with extracellular binding domains which mediate their interactions [3]. In the immune system, interactions between TNFR- and TNF-like proteins trigger a variety of signaling events which are critical for the initiation and regulation of immune responses, including T-cell/B-cell communication and activation and programmed cell death (apoptosis) [3,4]. Fas–FasL interactions play a fundamental role in the control of the immune response by initiating apoptosis [5]. Ligand binding to Fas on the cell surface transmits signals into Fas-expressing cells that trigger a cascade of cytoplasmic events which ultimately result in cellular degradation and death [5,6].

Three-dimensional (3D) structures of TNF-α [7] and -β [8], the CD40 ligand (CD40L, gp39) [9], TNFR [10], and the TNFR/TNF-β complex [11] have been determined by X-ray crystallography. These studies have elucidated the prototypic structural motifs shared by members of the TNFSF [9,11] and TNFRSF [12], respectively. These findings have made TNFSF and TNFRSF proteins attractive targets for comparative molecular modeling [12,13], despite limited sequence identity of ∼20–30%, and modeling studies have been reported on CD40 [14], Fas [15], RANK [16], CD40L [13,17,18], FasL [19], and the CD40–CD40L [18,20] and Fas–FasL [21] complexes. Some of these studies aided in mutagenesis analyses of receptor–ligand interactions. X-ray structure- and/or molecular model-

*To whom correspondence should be addressed at: MDS Panlabs, Computational Chemistry & Informatics, 11804 North Creek Pkwy. S., Bothell, WA 98011-8805, U.S.A.

based mutagenesis studies have been reported on TNF [22], CD40L [18,20], FasL [21], CD40 [18,20], and Fas [23,24]. Taken together, these studies have revealed that receptors and ligands employ largely non-conserved residues [24] in regions corresponding to the TNFR/TNF-β interface [11] to mediate their interactions. This supports the view that the TNFR/TNF-β complex provides a meaningful template for studying the interaction between other TNFR-like receptors and their TNF-like ligands [18,20,21].

Studies on the ligand binding site of Fas have provided an example for extensive structure–function analysis based on a molecular model. A comparative model of the extracellular TNFR-homologous region of Fas was generated based on the structure of TNFR [15]. The model was used to map conserved TNFRSF residues, outline the putative ligand binding site, and predict eight residues (K78, K84, R86, R87, L90, E93, H95, H126) as important for FasL recognition [15]. Subsequent mutagenesis analyses confirmed that six of these eight residues (except K78 and H95) were in fact important for FasL binding [23] and identified other important residues (R52, F81, F117) [24]. Mutations of these Fas residues significantly reduced or abolished ligand binding but did not measurably affect binding to a panel of conformationally sensitive monoclonal antibodies (mAbs), indicating that the mutant proteins were overall structurally sound. In the Fas model, residues important for ligand binding formed a coherent surface [24].

The identification of nine Fas [24] and two FasL [21] residues important for the Fas–FasL interaction suggested the analysis of this receptor–ligand interaction in more detail. Our previous studies were entirely based on a Fas molecular model and did not take information about the Fas ligand into account. Therefore, new molecular models of FasL, Fas, and the Fas–FasL complex were built, and the Fas–FasL model was used to analyze important Fas and FasL residues and likely effects of their mutation. Modeling studies at this level of detail are, in general, difficult due to inherent limitations of model building. Therefore, a conservative modeling protocol was applied and regions whose backbone conformations could not be predicted with confidence were deliberately omitted from the models. These regions included non-conserved loops and segments with insertions or deletions, which are, in addition to topological misalignments, major error sources in comparative protein models [25,26]. Thus, while not all regions of the Fas–FasL complex were modeled, the partial models were of higher prediction confidence and suitable for a more detailed analysis of important residues. The construction of the Fas, FasL, and Fas–FasL molecular models and the analysis of the Fas–FasL interface in the light of mutagenesis data are discussed herein. In the absence of X-ray data, the study extends our understanding of how Fas and its ligand interact at the molecular level of detail.

Methods

Sequences were aligned and structures were superimposed with the Align function of MOE (Molecular Operating Environment, v. 98.03, Chemical Computing Group, Montreal). MOE-Align uses a Needleman and Wunsch-like algorithm [27] for sequence alignments. In these calculations, the Gonnet matrix was applied [28]. In MOE, alignment of sequences can be combined with rigid-body superposition of structures using an iterative sequence and structure alignment procedure. This technique was used to generate a superposition-based sequence alignment of TNF-α, TNF-β, and CD40L, for which X-ray structures have been reported [7,9,11]. The alignment was inspected in detail and modified in a few regions to optimize the topological correspondence of residues. Based on the superposition, residues with α-carbon positions within 2 Å in TNF-α, TNF-β, and CD40L were determined by calculating pairwise α-carbon displacements and combined as structurally conserved regions. The sequence of the human Fas ligand was obtained from the SWISS-PROT [29] database (code P48023), and the extracellular TNF-homologous region was included in the sequence–structure alignment by matching consensus residues in core β-strands.

The FasL model was built using this alignment and receptor-bound TNF-β [11] as the template structure (Brookhaven Protein Data Bank (PDB) [30] code 1TNR). A new model of Fas was also generated based on TNFR in the TNFR/TNF-β complex [11] rather than using uncomplexed TNFR [10] as in our initial study [15]. This model was built following a previously generated structure-based alignment of TNFR, CD40, and Fas sequences from different species [15]. Although conformational differences between complexed and uncomplexed TNFR are subtle [10], modeling of both FasL and Fas based on 1TNR made it possible to avoid superposition errors in the assembly of the Fas–FasL complex. In addition to conserved core β-strands, short β-hairpins and backbone conformations of loops with the same length and conserved

sequences were retained in the molecular models. Ab initio modeling of regions including insertions and deletions and non-conserved loops, which are particularly prone to modeling errors [25,26], was avoided, and these regions were omitted from the models. This conservative approach, focusing on structural conservation, was thought to produce more accurate, albeit incomplete, molecular models, thereby avoiding significant errors in the subsequent analysis of the Fas–FasL interface.

Interactive model building and computer graphical analysis were carried out using InsightII and its Biopolymer module (v. 97.0, MSI, San Diego, CA). Figures were also generated with InsightII. Residue replacements were carried out using rotamer conformations [31] following the original side-chain path if possible. Alternatively, substitutions were modeled by a search procedure for low-energy rotamers [32] as implemented in InsightII. The stereochemistry and intramolecular contacts of the Fas and FasL models were refined by limited conjugate gradient energy minimization using MOE (for details, see Labute, P., MOE Forcefield Facilities, on-line article, Journal of the Chemical Computing Group; http://www.chemcomp.com). As a consequence of energy refinement, backbone root mean square (rms) deviations from the template structures were ∼0.5 Å. The molecular models were evaluated with PROCHECK [33] and displayed good stereochemistry and intramolecular contacts. The model of the Fas–FasL complex showed only minor steric problems at the interface which could be corrected without the need for more extensive energy minimization by generating a few alternative side chain conformations. Significant errors in the Fas and FasL models should be limited to incorrectly placed side chains. Therefore, alternative rotamer conformations were also generated and evaluated for potential contact residues during the analysis of receptor–ligand interactions.

Results and discussion

Structural prototypes

The template structures for model building are shown in Figure 1. The prototypic fold of TNFR consists of an elongated repeat domain with a limited hydrophobic core that is stabilized by canonical disulfide bonds in a ladder-like arrangement [11]. The structures of the first three repeat domains in TNFR are well conserved [10,11] and consist of conserved modules [12]. The extracellular regions of TNFRSF proteins include a varying number of repeat domains. In contrast to TNFR, the TNF fold consists of a sandwich of two β-sheets with jelly roll topology and an extensive hydrophobic core [7–9]. TNF-like monomers expose conserved hydrophobic residues on their surface and form a symmetrical homotrimer [7–9]. The sequences of both TNFRSF [11,14] and TNFSF [13,17] proteins display characteristic sequence motifs. Many of these conserved residues are important for the integrity of their respective 3D structures. In the TNFR/TNF-β complex, a receptor molecule binds to the interface between two adjacent monomers of the homotrimeric ligand [11]. Ligand binding thus leads to receptor trimerization, and the complex contains three equivalent, independent, and symmetrically arranged receptor–ligand interfaces [11].

TNFSF structure comparison

To aid in the modeling of FasL, the X-ray structures of TNF-α [7] (PDB code 1TNF), TNF-β [11] (1TNR), and CD40L [9] (1ALY) were compared and structurally conserved regions were identified. After optimal superposition with MOE, residues with α-carbon positions within 2 Å in the three structures were determined. Structurally conserved regions include, but are not limited to, the majority of residues in core β-strands. Figure 2 shows the superposition of these structures and illustrates that core regions superpose closely, whereas large deviations are observed in loop regions, which are difficult to model [26]. Figure 3 shows the sequence alignment that corresponds to the superposition. The topological alignment made it possible to unambiguously align the FasL sequence with structural templates.

FasL molecular model

The FasL sequence was included in the alignment by matching consensus residues in structurally conserved regions (Figure 3). These consensus residues largely correspond to conserved residues in β-strands which participate in the formation of the extensive hydrophobic core. The conservation of these core residues makes it possible to align the sequences of TNF-like proteins with high confidence, despite overall low sequence identity. In the aligned region, the FasL sequence is most identical to TNF-β (∼28%), followed by TNF-α (∼25%), and CD40L (∼21%). Therefore, TNF-β was selected as structural template for model building, and the identified structurally conserved regions were copied to the FasL model. Also

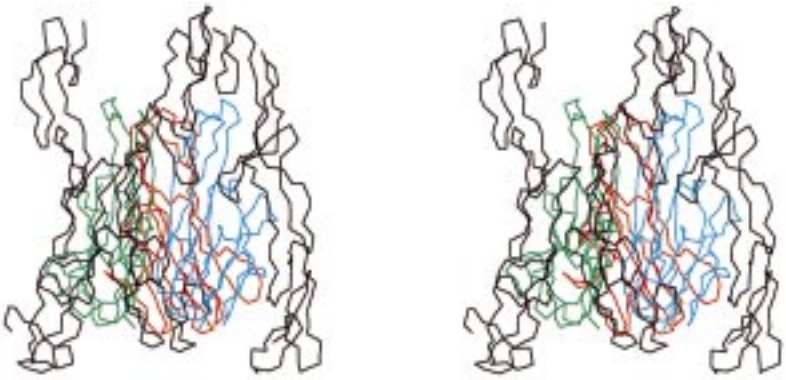

Figure 1. Structural templates. Stereoview of the α-carbon trace of the X-ray structure of the TNFR/TNF-β complex. TNFR is shown in black and TNF-β monomers are colored red, blue, and green, respectively.

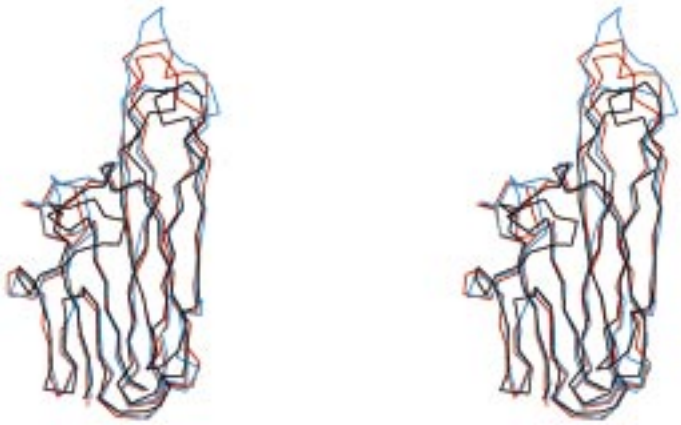

Figure 2. Comparison of TNFSF structures. Stereoview of the α-carbon superposition of TNF-β (red), TNF-α (blue), and CD40L (black) monomers.

included in the FasL model were other regions conserved in TNF-β and FasL, e.g., the four-residue loop connecting strands d and e (SQYP versus SKYP) (Figure 3). After matching hydrophobic consensus residues, the alignment of FasL residues 144–281 relative to TNF proteins and CD40L did not contain ambiguous regions. However, residues forming nonconserved loop regions (residues 151–159, 165–167, 171–172, 200–206, 230–238, 269–271) were omitted from the FasL model, since conformations of these regions are difficult to model with confidence. Thus, the model represents a compromise of modeling accuracy and completeness. Figure 4 shows a schematic representation of the model with tentative conformations included for those regions that were omitted from the final model.

Fas molecular model

In contrast to TNF proteins, TNFR is presently the only representative of the TNFRSF with experimentally determined structure. Therefore, it is important to include multiple sequences of TNFR-like proteins in the initial alignment so that conservation of structural key residues can be better detected. The extracellular region of Fas includes three TNFR-like repeat domains. The sequence alignment in Figure 5 was used as the basis for model building and shows that these domains can be unambiguously aligned with the first three domains in TNFR by matching canonical cysteine positions and other conserved residues [11] in each domain [15]. In the aligned region, the sequence identity between human Fas and TNFR is ∼24%. Our previous Fas model [15] was built based on uncomplexed TNFR [10] using comparative modeling techniques [13] complemented by conformational search [34]. Here the model was constructed based

```
CD40L      QIAAHVISEASSKTTSVLQWAEKGY-YTMSNNLVTLENG
TNFA       KPVAHVVANPQ--AEGQLQWLNRRANALLAN-GVELRD-
TNFB       KPAAHLIGDP-SK-QNSLLWRANTDRAFLQD-GFSLSN-
FASL  144  RKVAHLTGKSNSR-SMPLEWEDTYG-IVLLS-GVKYKK-  178
              aaaa             aa'     aaa''  bbb'

CD40L      KQLTVKRQGLYYIYAQVTFCSN----REASSQAPFIASLCLKS
TNFA       NQLVVPSEGLYLIYSQVLFKGQG----CPSTHVLLTHTISRIA
TNFB       NSLLVPTSGIYFVYSQVVFSGKAYSPKATSSPLYLAHEVQLFS
FASL  179  GGLVINETGLYFVYSKVYFRGQS------CNNLPLSHKVYMRN  215
            bbbb    ccccccccccccc          ddddddddddd

CD40L      -PGRFERILLRAANTHSSAKP--------CGQQSIHLGGVFEL
TNFA       VSYQTKVNLLSAIKSPCQRETPEGAEAKPWYEPIYLGGVFQL
TNFB       SQYPFHVPLLSSQKMVYPG------LQEPWLHSMYHGAAFQL
FASL  216  SKYPQDLVMMEGKMMSYCT------TGQMWARSSYLGAVFNL  251
                 eeeeeeeeee              fffffffffffff

CD40L      QPGASVFVNVTDPSQVS-HGTGFTSFGLLKL
TNFA       EKGDRLSAEINRPDYLLFAESGQVYFGIIAL
TNFB       TQGDQLSTHTDGIPHLV-LSPSTVFFGAFAL
FASL  252  TSADHLYVNVSELSLVN-FEESQTFFGLYKL  281
              ggggggggg              hhhhhhh
```

Figure 3. Alignment of TNFSF sequences. The extracellular region sequence of the human Fas ligand (FASL) was aligned with CD40L, TNF-α (TNFA), and TNF-β (TNFB). The alignment is based on superposition of X-ray structures (Figure 2). Structurally conserved regions are underlined and β-strands in TNF-β are labeled a–h. Residues conserved in all sequences are shown in bold and residue numbers are given for FASL.

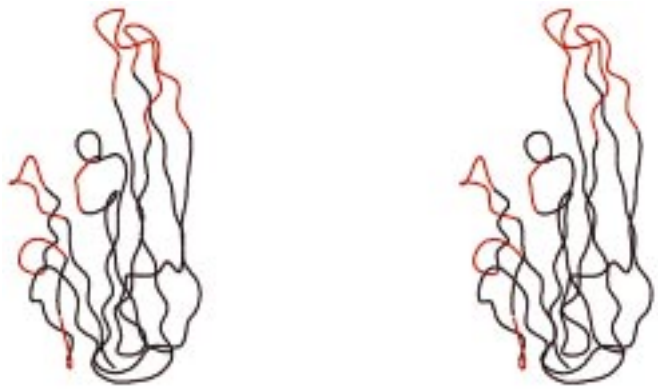

Figure 4. FasL molecular model. An outline of the monomer is shown with tentative regions not included in the final model colored red.

on ligand-bound TNFR [11] and ab initio modeling techniques were not applied. The targeted region includes residues 47–149, i.e., the third disulfide loop of the N-terminal TNFR-like domain and domains 2 and 3, but non-conserved segments (residues 57–64, 71–74, 119–125, 134–136) were not modeled. Figure 6 shows a comparison of the two Fas molecular models. The α-carbon rms deviation after superposition of the models was ∼1.3 Å. Thus, conformational differences were subtle. In the current Fas model, only one disulfide loop of the N-terminal TNFR-like domain was modeled because other parts of this domain were disordered in the X-ray structure of ligand-bound TNFR used as template. Modeling of these regions was also not necessary since they are distant from the Fas–FasL interface analyzed here. In the N-terminal domain of Fas, two of the canonical cysteine residues are not conserved, making it difficult to predict the disulfide bond pattern with confidence. It was suggested previously that the formation of an alternative disulfide bond in the N-terminal domain of Fas is possible without substantial structural changes [15].

Fas–FasL complex

The relative orientation of Fas and FasL closely resembles the TNFR/TNF-β complex [11] because the complex was used as the template structure. Supported by the results of mutagenesis, the TNFR/TNF-β complex serves as a prototype for other TNFRSF/TNFSF interactions [18,21]. Figure 7 shows one of the three equivalent receptor–ligand interfaces in the Fas–FasL complex, consisting of two adjacent FasL monomers and Fas, that was used to map important residues and study receptor–ligand interactions. Due to the absence of speculative regions, only minor steric problems were observed at the Fas–FasL interface, which were corrected by adjusting the side chain conformations of a few residues. Superposition of the original Fas model on the complex resulted, despite the relatively low rms deviation between the two Fas models, in considerably more unfavorable contacts. This was due to the presence of speculative loop conformations in Fas and subtle changes in the overall orientation of Fas relative to FasL. These findings supported the use of the new Fas model in the subsequent analysis. Fas contains N-linked glycosylation sites at residues 102 and 120, and FasL contains glycosylation sites at residues 184, 250, and 260. In the following, FasL residues are labeled 'fl' to distinguish them from residues in Fas (e.g., N184 in FasL is N184fl). With the exception of N120, which is part of a loop not included in the model, all glycosylation sites could be mapped. Figure 7 shows that the potential N-linked glycosylation sites in both Fas and FasL map to positions at the periphery or outside the receptor–ligand interface so that attached glycans, if present, would not interfere with binding. The sequence alignments in Figures 3 and 5 show that N-linked glycosylation sites are generally not conserved in TNF- and TNFR-like proteins. Only the N-linked glycosylation site at position 260 in FasL is conserved in CD40L but not in TNF-α or -β.

Mapping of residues important for binding

In Fas, a total of nine residues were identified as important for FasL binding (R52, F81, K84, R86, R87, L90, E93, F117, H126), the majority of which are part of the central domain two [23,24]. Mutation of these residues, typically to serine, significantly reduced or abolished binding to FasL but not to a panel of conformationally sensitive mAbs, suggesting the absence of large structural perturbations as a consequence of mutation. Another mutagenesis study on FasL identified two residues (P206fl, Y218fl) involved in Fas binding [21]. These two residues were also analyzed using a molecular model [21], generated by an automatic modeling procedure [35], but details concerning the modeling were not provided. How many critical residues could be mapped and analyzed using our Fas–FasL model? All nine Fas residues and Y218fl, but not P206fl, were part of the modeled regions (Figure 7). However, residues K84, R87, L90, and H126 were excluded from further analysis because they interacted closely and, in part, exclusively with segments in FasL that could not be confidently predicted and were not included in the final model. Thus, specific interactions involving these four residues could not be analyzed. The remaining six of 11 residues (five in Fas and one in FasL) were analyzed in detail.

Table 1. Contacts between Fas and FasL residues discussed in the text

Fas residue	FasL residue	Distance (Å)
K78 CB	Y218fl CE1	4.0
F81 CE1	S216fl O	3.1
F81 CD1	K217fl CA	3.8
R86 NH1	V223fl O	3.4
R87 NH1	E163fl OE1	2.9
R87 NH1	E163fl OE2	3.1
R89 NH1	E226fl OE2	3.8
R89 NH2	E226fl OE1	3.1
D92 OD1	N268fl ND2	4.1
D92 OD2	K228fl NZ	4.2
E93 OE1	R198fl NH1	3.2
E93 OE1	R198fl NH2	2.7

Analysis of Fas–FasL interactions

When mapped on the Fas model, residues implicated in binding form a coherent ligand binding surface (Figure 7). Computer graphical analysis of the modeled Fas–FasL interface made it possible to differentiate between the importance of these residues and to identify other contact residues. Residue F117 is too distant from the interface to interact with FasL directly. Thus, mutation of this residue to serine (F117S) probably caused subtle structural perturbations not detectable by mAb binding profiles but sufficient to compromise the Fas–FasL interaction. Mutation of R52 to serine also resulted in wild-type-like mAb binding profiles. The side chain of R52 is involved in packing interactions with other Fas residues, but its guanidino group is exposed and in contact distance to FasL. It is therefore difficult to decide whether the mutation

```
DI                CC1                 CC1 CC2 CC3          CC2       CC3
                   *     *             *   **  *             *      ** *
TNFR Human   SVCPQGK YIHPQNNSI   C    CTK CHKGTYLYND  CPGPGQDTDCR
TNFR Mouse   SLCPQGK YVHSKNNSI   C    CTK CHKGTYLVSD  CPSPGRDTVCR

FAS  Human   TQNLEGL H---HDGQF   C    HKP CPPGERKARD  CTVNGDEPDCV
FAS  Mouse   KNCSEGL Y---QGGPF   C    CQP CQPGKKKVED  CKMNGGTPTCA
             30             40                50          60
CD40 Human   TACREKQ YLI---NSQ   C    CSL CQPGQKLVSD  CTE-FTETECL
CD40 Mouse   VTCSDKQ YLH---DGQ   C    CDL CQPGSRLTSH  CTA-LEKTQCH


DII
                   *     *             *   **  *             *      ** *
TNFR HUMAN   E CESG-SFTASENHLRH CLS CSK CRKEMGQVEISSCTVDR DTVCG
TNFR Mouse   E CEKG-TFTASQNYLRQ CLS CKT CRKEMSQVEISPCQADK DTVCG

FAS  Human   P CQEGKEYTDKAHFSSK CRR CRL CDEGHGLEVEINCTRTQ NTKCR
FAS  Mouse   P CTEGKEYMDKNHYADK CRR CTL CDEEHGLEVETNCTLTQ NTKCK
               70        80           90          100         110
CD40 Human   P CGES-EFLDTWNRETH CHQ HKY CDPNLGLRVQQKGTSET DTICT
CD40 Mouse   P CDSG-EFSAQWNREIR CHQ HRH CEPNQGLRVKKEGTAES DTVCT


DIII
                   *     *             *   **  *             *      ** *
TNFR Human     CRKNQ YRHYWSENLFQCFN CSL CLNG-TVHLS  CQEKQ NTVCT
TNFR Mouse     CKENQ FQRYLSETHFQCVD CSP CFNG-TVTIP  CKETQ NTVCN

FAS  Human     CKPNF FCNSTV--CEHCDP CTK CEHG--IIKE  CTLTS NTKCK
FAS  Mouse     CKPDF YCDSPG--CEHCVR CAS CEHG--TLEP  CTATS NTNCR
                       120           130           140           150
CD40 Human     CEEGW HCTSEA--CESCVL HRS CSPGFGVKQI  ATGVS DTICE
CD40 Mouse     CKEGQ HCTSKD--CEACAQ HTP CIPGFGVMEM  ATETT DTVCH
```

Figure 5. Alignment of TNFRSF sequences. The three N-terminal repeat domains (DI, DII, DIII) of TNFR, CD40, and FAS were aligned with respect to cysteines forming canonical disulfide bonds (CC1, CC2, CC3), and other TNFRSF signature residues (∗). Residue numbers are given for Fas.

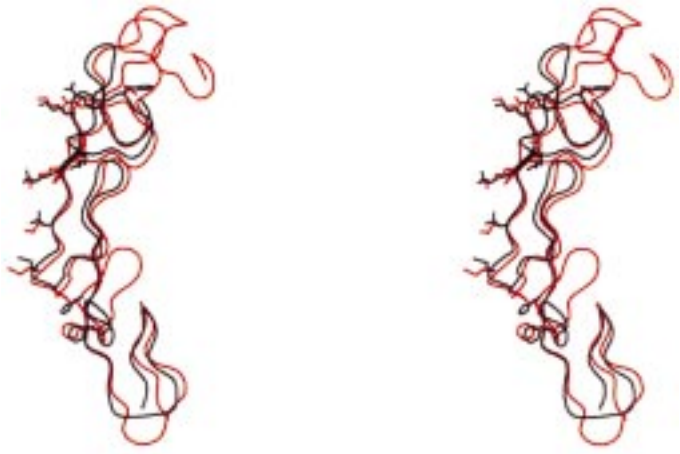

Figure 6. Molecular models of Fas. Shown is an outline of the original (red) and partial (black) Fas model after superposition. In this orientation, the N-terminal domain is at the top. The side chains of residues important for ligand binding are shown in both models.

R52S affected Fas structure or FasL binding directly. Other residues were found to be involved in specific receptor–ligand interactions which are summarized in Table 1. Residues E93 and R198fl form an ionic interaction across the interface which explains the observed importance of E93 for binding. The model displayed two other attractive charge–charge interactions between receptor and ligand, both of which

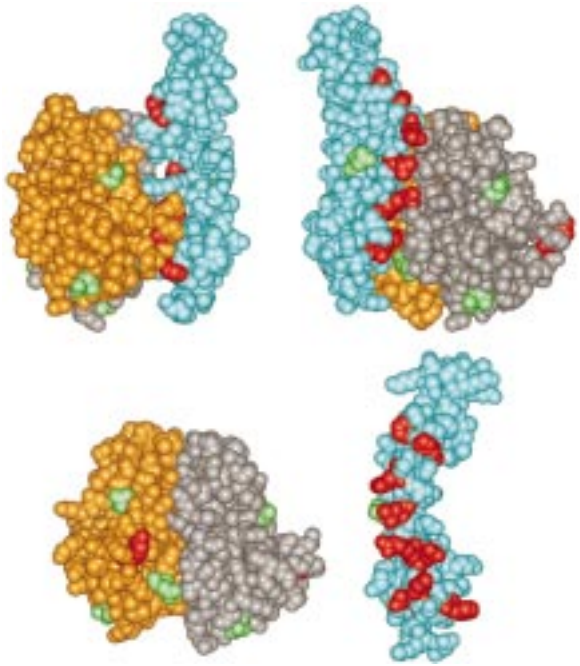

Figure 7. Fas–FasL molecular model. The receptor–ligand interface is shown as a space-filling model. FasL monomers are colored gold and silver, respectively, and Fas is colored blue. Glycosylation sites are green and residues implicated in binding by mutagenesis are red. At the top, the complex is shown in two orientations, related by ~180° rotation around the vertical axis. At the bottom, the complex was opened like a book so that the view is facing the contact area.

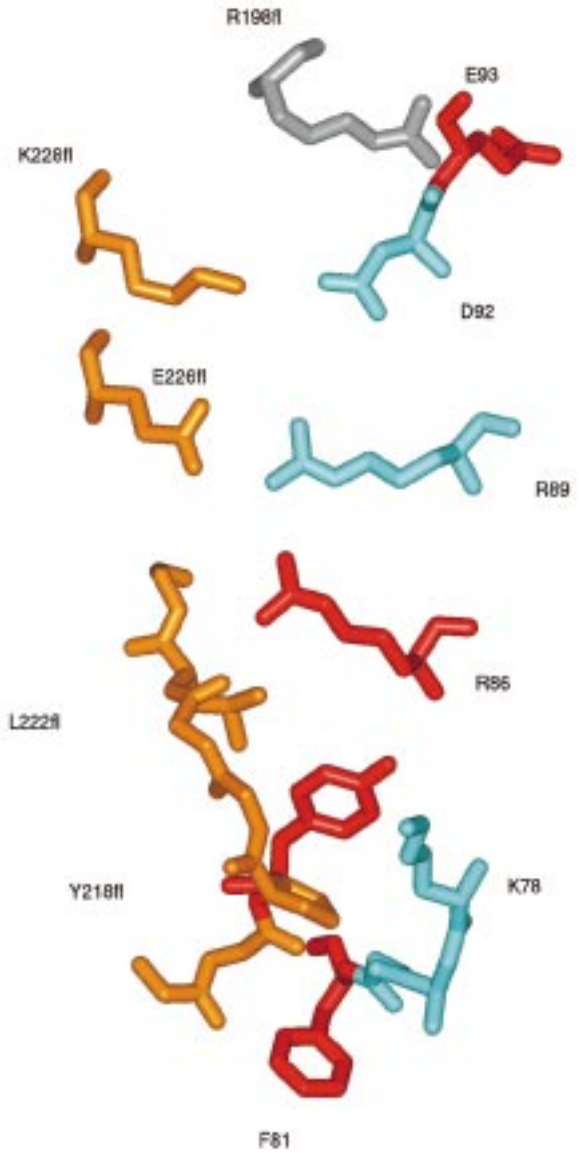

Figure 8. Fas–FasL interactions. Residues at the receptor–ligand interface are shown. The orientation is similar to the top left view of Figure 7 and the same color code is used.

involve previously unidentified residues, D92–K228fl and R89–E226fl. Figure 8 shows the array of salt bridges at the 'upper' part of the interface. R86 which is, like R87, essential for ligand binding [23] is the most centrally located residue at the interface, and its replacement by a serine residue creates a 'hole' and severely affects surface complementarity. Dependent on its rotamer conformation, R86 can interact with side chain and main chain carbonyl oxygen atoms of several residues (Y218fl, L222fl, V223fl). When Y218fl was mutated and implicated in Fas binding, an interaction between Y218fl and R86 was also proposed [21]. A reason for this prediction was the finding that mutant protein Y218flD was active at wild-type levels in cytotoxic assays, whereas Y218flR was inactive, consistent with the idea that Y218flD, i.e., a negatively charged residue at this position, would favorably interact with R86 [21]. The present study suggests an alternative explanation for the observed importance of Y218fl. In the model, Y218fl fills a cavity between loops S216fl–P219fl and K78–F81 and is close to residue K78. Although K78 is, on the basis of mutagenesis, not important for FasL binding [24], the introduction of a positive charge close to this residue, as in Y218flR, is likely to affect the Fas–FasL interaction. Another important Fas residue, F81, maps to the same region. The side chain of this residue closely packs against the S216fl–P219fl loop, consistent with its role in binding. In Figure 8, the interactions at the 'lower' part of the interface are also shown. As described above, interactions between charged residues are thought to play an important role in ligand binding

to Fas, similar to CD40 [20]. Thus, while protein–protein interactions often depend on the formation of large hydrophobic interfaces, analyses of Fas–FasL and CD40–CD40L interactions suggest a critical role of electrostatic effects. This may perhaps be a characteristic and specificity determining feature of TNFRSF/TNFSF interactions on the cell surface. What are the implications for ligand design? The absence of distinct hydrophobic binding pockets in both Fas and FasL and the presence of electrostatic interactions widely distributed over the interface suggest that it may be difficult to generate small molecular inhibitors to specifically block the Fas–FasL interaction.

Conclusions

This study focused on the construction and analysis of a 'less complete/more accurate' Fas–FasL model by deliberately excluding regions for which no conserved backbone templates were identified. This was done to reduce modeling errors which are particularly critical when analyzing molecular interactions. The present modeling study, taking FasL into account, has provided a more differentiated picture of the role of Fas and FasL residues implicated in binding. Although specific interactions involving residues K84, R87, L90, and H126 could not be analyzed, these residues are, based on their positions, very likely to participate in the formation of the receptor–ligand interface, consistent with mutagenesis results. Interactions involving six other residues (R52, F81, R86, E93, F117, Y218fl) could be studied in detail. Mutation of F117 and R52 probably caused some structural perturbations proximal to the interface. However, residues F81, R86, E93, and Y218fl were found to be involved in specific receptor–ligand contacts. Furthermore, five previously not targeted residues (D92, R89, R198fl, E226fl, K228fl) were identified as likely contact residues, forming electrostatic interactions between receptor and ligand.

Coordinates of the Fas–FasL molecular model have been deposited in the Brookhaven Protein Data Bank (PDB ID code '1bzi').

References

1. Itoh, N., Yonehara, S., Ishii, A., Yonehara, M., Mizushima, S.-I., Sameshima, M., Hase, A., Seto, Y. and Nagata, S., Cell, 66 (1991) 233.
2. Suda, T., Takahashi, T., Golstein, P. and Nagata, S., Cell, 75 (1994) 1169.
3. Beutler, B. and van Huffel, C., Science, 264 (1994) 667.
4. Smith, C.A., Farrah, T. and Goodwin, R.G., Cell, 76 (1994) 959.
5. Nagata, S. and Golstein, P., Science, 267 (1995) 1449.
6. Nagata, S., Adv. Exp. Med. Biol., 406 (1996) 119.
7. Eck, M.J. and Sprang, S.R., J. Biol. Chem., 264 (1989) 17595.
8. Eck, M.J., Ultsch, M., Rinderknecht, E., de Vos, A.M. and Sprang, S.R., J. Biol. Chem., 267 (1992) 2119.
9. Karpusas, M., Hsu, Y.-M., Wang, J.-H., Thompson, J., Lederman, S., Chess, L. and Thomas, D., Structure, 3 (1995) 1031.
10. Naismith, J.H., Devine, T.Q., Brandhuber, B.J. and Sprang, S.R., J. Biol. Chem., 270 (1995) 13303.
11. Banner, D.W., D'Arcy, A., Janes, W., Gentz, R., Schoenfeld, H.-J., Broger, C., Loetscher, H. and Lesslauer, W., Cell, 73 (1993) 431.
12. Naismith, J.H. and Sprang, S.R., Trends Biochem. Sci., 23 (1998) 74.
13. Bajorath, J., Stenkamp, R. and Aruffo, A., Protein Sci., 2 (1993) 1798.
14. Bajorath, J. and Aruffo, A., Proteins Struct. Funct. Genet., 27 (1997) 59.
15. Bajorath, J. and Aruffo, A., J. Comput.-Aided Mol. Design, 11 (1997) 3.
16. Bajorath, J., J. Mol. Model., 4 (1998) 239. 17.
17. Peitsch, M.C. and Jongeneel, C.V., Int. Immunol., 5 (1993) 233.
18. Bajorath, J., Marken, J.S., Chalupny, N.J., Spoon, T.L., Siadak, A.W., Gordon, M., Noelle, R.J., Hollenbaugh, D. and Aruffo, A., Biochemistry, 34 (1995) 9884.
19. Peitsch, M.C. and Tschopp, J., J. Mol. Immunol., 32 (1995) 761.
20. Singh, J., Garber, E., Van Vlijmen, H., Karpusas, M., Hsu, Y.-M., Zheng, Z., Naismith, J.H. and Thomas, D., Protein Sci., 7 (1998) 1124.
21. Schneider, P., Bodmer, J.-L., Holler, N., Mattmann, C., Scuderi, P., Terskikh, A., Peitsch, M.C. and Tschopp, J., J. Biol. Chem., 272 (1998) 18827.
22. van Ostade, X., Tavernier, J. and Fiers, W., Protein Eng., 7 (1994) 5.
23. Starling, G.C., Bajorath, J., Emswiler, J., Ledbetter, J.A., Aruffo, A. and Kiener, P.A., J. Exp. Med., 185 (1997) 1487.
24. Starling, G.C., Kiener, P.A., Aruffo, A. and Bajorath, J., Biochemistry, 37 (1998) 3723.
25. Martin, A.C., MacArthur, M.W. and Thornton, J.M., Proteins Struct. Funct. Genet. Suppl., 1 (1998) 14.
26. Bajorath, J., J. Biol. Chem., 273 (1998) 24603.
27. Needleman, S.B. and Wunsch, C.D., J. Mol. Biol., 48 (1970) 443.
28. Gonnet, G.H., Cohen, M.A. and Benner, S.A., Science, 256 (1992) 1433.
29. Bairoch, A. and Apwiler, R., Nucleic Acids Res., 26 (1998) 38.
30. Bernstein, F.C., Koetzle, T.F., Williams, G.J.B., Meyer, E.F., Jr., Brice, M.D., Rodgers, J.R., Kennard, O., Shimanouchi, T. and Tasumi, M., J. Mol. Biol., 112 (1977) 535.

31. Ponder, J. W. and Richards, F. M., J. Mol. Biol., 193 (1987) 775.
32. Bajorath, J. and Fine, R. M., Immunomethods, 1 (1992) 137.
33. Laskowski, R.A., MacArthur, M.W., Moss, D.S. and Thornton, J.M., J. Appl. Crystallogr., 26 (1993) 283.
34. Bruccoleri, R.E. and Novotny, J., Immunomethods, 1 (1992) 96.
35. Peitsch, M. C., Biotechnology, 13 (1995) 658.